Acta Biochim Biophys Sin 2010, 42: 440–449 | © The Author 2010. Published by ABBS Editorial Office in association with Oxford University Press on behalf of the Institute of Biochemistry and Cell Biology, Shanghai Institutes for Biological Sciences, Chinese Academy of Sciences. DOI: 10.1093/abbs/gmq040.
Advance Access Publication 8 June 2010

Original Article

DNA binding, cytotoxicity, and apoptotic-inducing activity of ruthenium(II) polypyridyl complex

Peng Zhang, Jie Chen, and Yi Liang*

State Key Laboratory of Virology, College of Life Sciences, Wuhan University, Wuhan 430072, China
*Correspondence address. Tel/Fax: +86-27-68754902; E-mail: liangyi@whu.edu.cn

There is considerable interest in the interactions of ruthenium (Ru)(II) complexes with DNA as well as the biological impact of the interactions. Here, by using isothermal titration calorimetry, viscosity measurement, and circular dichroism, we investigated the interactions of a new Ru(II) complex, $[Ru(dmp)_2PMIP]^{2+}$ {dmp = 2,9-dimethyl-1,10-phenanthroline, PMIP = 2-(4-methylphenyl)imidazo [4,5-f]1,10-phenanthroline}, with calf thymus DNA (CT DNA). The Ru(II) polypyridyl complex and CT DNA formed a tight 1:1 complex with a binding constant of exceeding $10^6\ M^{-1}$ and with a binding mode of intercalation. Cell viability experiments indicated that the Ru(II) complex showed significant dose-dependent cytotoxicity to human lung tumor cell line A549. Further flow cytometry experiments showed that the cytotoxic Ru(II) complex induced apoptosis of human lung cancer cell line A549. Our data demonstrated that the Ru(II) polypyridyl complex binds to DNA and thereby induces apoptosis in tumor cells, suggesting that anti-tumor activity of the Ru(II) complex could be related to its interaction with DNA.

Keywords binding affinity; isothermal titration calorimetry; molecular recognition; cytotoxicity; apoptosis

Received: December 2, 2009 Accepted: April 10, 2010

Introduction

There is considerable interest in the interactions of ruthenium Ru(II) complexes with DNA as well as the biological impact of the interactions [1–7]. Ru(II) complexes are usually used as DNA structural probes, artificial nucleases, DNA molecular light switches, and DNA-targeting drugs [1–5]. Researches on anti-tumor active platinum complexes have always been a stimulating topic in decades [4,8,9]. Some Ru(II) complexes are structural analogues of transplatinum and cisplatin complexes and show promising anti-tumor activity [10,11]. Although the cytotoxicity of some Ru(II) complexes to tumor cells has been reported [10–13], the potential ability of Ru(II) complexes inducing apoptosis in tumor cells has been little documented.

In recent years, isothermal titration calorimetry (ITC) has become a widely used method for understanding molecular recognition within cells [14–18]. This method has yielded some useful thermodynamic data on the interactions of metal complexes with DNA [7,17,18], and assessing drug–DNA interaction is of great importance for drug development. In the present study, we employed ITC, viscosity measurement, equilibrium dialysis, and circular dichroism (CD) to investigate the interaction of a new Ru(II) complex, $[Ru(dmp)_2PMIP]^{2+}$ {dmp = 2,9-dimethyl-1,10-phenanthroline, PMIP = 2-(4-methylphenyl)imidazo [4,5-f]1,10-phenanthroline} (**Fig. 1**), a structural analogue of platinum complex, with calf thymus DNA (CT DNA), and then investigated the impact of the Ru(II) complex on human lung cancer cells A549, in order to further understand the binding mechanism and the biological impact of the interactions. The Ru(II) complex contains a PMIP-intercalating ligand and two dmp (2,9-dimethyl-1,10-phenanthroline) ancillary ligands. Because of the steric hindrance exerted by the methyl groups located at such ligands, we speculated that complex $[Ru(dmp)_2PMIP]^{2+}$ should be a moderate intercalative complex. The experimental results indicated that the Ru(II) complex and CT DNA formed a tight 1:1 complex with a binding constant exceeding $10^6\ M^{-1}$ and with a binding mode of intercalation, and suggested that anti-tumor activity of the Ru(II) complex could be related to its interaction with DNA.

Materials and Methods

Materials

CT DNA (Sigma-Aldrich, St Louis, USA) was dissolved in the corresponding buffer with appropriate concentration and stored at 4°C, then used not more than 1 day. CT DNA was purified by ethanol precipitation and centrifugal dialysis before use. The concentration of CT DNA solution

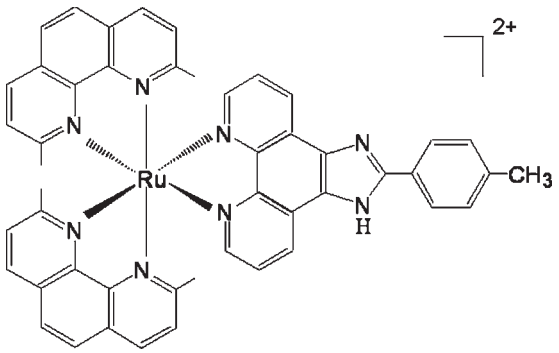

Figure 1 Structure of complex $[Ru(dmp)_2PMIP]^{2+}$

was determined spectroscopically at 260 nm using a molar extinction coefficient of 6600 M^{-1} cm^{-1} [19] and expressed as base concentrations throughout this paper. In all experiments, unless otherwise specified, CT DNA samples ~20,000 bp in average length were employed. 3-(4,5-Dimethylthiazol-2-yl)-2,5-diphenyltetrazolium bromide (MTT), trypan blue dye, propidium iodide (PI), and RNase were purchased from Sigma-Aldrich. All other chemicals used were made in China and of analytical grade. Tris–HCl buffer (5 mM, pH 7.2) containing 50 mM NaCl was used for viscosity measurements and CD spectroscopic studies. Because the heat effects of ionization and dilution of Tris–HCl buffer were too large to measure the binding heat effect exactly, 20 mM HEPES (Amresco Chemical Co., Solon, USA) buffer, pH 7.2, containing 0.1 mM EDTA was used for ITC experiments.

Synthesis of $[Ru(dmp)_2PMIP](ClO_4)_2$

1,10-Phenanthroline-5,6-dione and *cis*-$[Ru(dmp)_2Cl_2]\cdot 2H_2O$ were prepared according to the literature procedures [20]. PMIP was synthesized by a method similar to that described previously [21]. Briefly, a mixture of 4-methylbenzaldehyde (3.5 mmol, 0.41 ml), 1,10-phenanthroline-5,6-dione (2.5 mmol, 0.525 g), ammonium acetate (50 mmol, 3.88 g), and glacial acetic acid (10 ml) was refluxed for about 2 h, cooled to room temperature, and diluted with water (about 25 ml). Dropwise addition of concentrated aqueous ammonia gave yellow precipitates, which were collected and washed with water. The crude products were purified by silica gel filtration (60–100 mesh, ethanol). The principal yellow band was collected. The solvent was removed by rotary evaporation, and the products were collected and dried at 50°C *in vacuo*. Yield was 0.464 g, 60%.

Complex $[Ru(dmp)_2PMIP](ClO_4)_2$ (red) was prepared by the following method. Briefly, a mixture of *cis*-$[Ru(dmp)_2Cl_2]\cdot 2H_2O$ (0.5 mmol, 0.321 g), PMIP (0.5 mmol, 0.155 g), ethanol (10 ml), and water (5 ml) was refluxed under argon for 2 h to give a clear red solution. After most of the ethanol solvent was removed under reduced pressure, a red precipitate was obtained by dropwise addition of a saturated aqueous $NaClO_4$ solution. The product was purified by column chromatography on alumina using acetonitrile–toluene (1:1, v/v) as an eluent and then dried *in vacuo*. Yield was 0.360 g, 70%. Characterization data of PMIP are as follows: Anal. Found: C, 77.26; H, 4.63; N, 17.92%. Calc. for $C_{20}H_{14}N_4$: C, 77.42; H, 4.52; N, 18.06%. ^{1}H NMR (DMSO-d_6): δ 13.56 (br, 1H), 9.03 (d, 2H), 8.95 (d, 2H), 8.21 (d, 2H), 7.82 (q, 2H), 7.41 (d, 2H), 2.42 (s, 3H). *m/z* 311 ($[M+1]^+$). For $[Ru(dmp)_2PMIP](ClO_4)_2$: Anal. Found: C, 56.03; H, 3.80; N, 10.87%. Calc. for $C_{48}H_{38}Cl_2N_8O_8Ru$: C, 56.14; H, 3.70; N, 10.92%. ^{1}H NMR (DMSO-d_6): δ 8.90 (d, 2H), 8.80 (d, 2H), 8.43 (t, 4H), 8.24 (d, 2H), 8.15 (d, 2H), 7.97 (d, 2H), 7.38 (m, 4H), 7.32 (d, 2H), 7.22 (br, 2H), 2.29 (s, 3H), 1.83 (s, 3H), 1.70 (s, 6H). *m/z* 827 ($[M-2ClO_4^-]^{2+}$).

Isothermal titration calorimetry

ITC experiments on the interactions of Ru(II) complex with CT DNA in HEPES buffer (20 mM, containing 0.1 mM EDTA, pH 7.2) were carried out at 20.0, 25.0, 30.0, and 37.0°C using an isothermal titration calorimeter (VP-ITC; MicroCal, Northampton, USA) with stirring at 300 rpm. About 1.43 ml of CT DNA solution was titrated with the complex solution. A typical titration experiment consisted of 28 consecutive injections of 10-μl volume and 20-s duration each, with a 5-min interval between injections. Heats of dilution of the complex were determined by injecting the complex solution into the buffer alone and the total observed heats of binding were corrected for the heat of dilution. MicroCal ORIGIN software was used to determine the site-binding model that gave a good fit (low χ^2 value) to resulting data. From the various binding models tested (a single set of identical sites model, two sets of independent sites model, and sequential binding sites model), only the single set of identical sites model fitted adequately to the binding isotherms, and the standard molar enthalpy change for the binding ($\Delta_b H_m^0$), the binding constant (K_b), and the binding stoichiometry (n) were thus obtained. The standard molar free energy change ($\Delta_b G_m^0$) and the standard molar entropy change ($\Delta_b S_m^0$) for binding reaction were calculated by the fundamental equations of thermodynamics [22] as Equations (1) and (2):

$$\Delta_b G_m^0 = -RT \ln K_b \quad (1)$$

$$\Delta_b S_m^0 = \frac{(\Delta_b H_m^0 - \Delta_b G_m^0)}{T} \quad (2)$$

The molar heat capacity change associated with the binding of Ru(II) complex to CT DNA ($\Delta_b C_{P,m}$) was obtained by linear regression analysis of the plots by $\Delta_b H_m^0 = \Delta_b C_{P,m} T + \Delta H^0$ and $\Delta_b S_m^0 = \Delta_b C_{P,m} \ln T + \Delta S^0$,

respectively. Here, ΔH^0 and ΔS^0 are constants of linear fitting.

Viscosity measurements

Viscosity experiments were carried out using an Ubbelodhe viscometer (Sangli, Nanjing, China) maintained at 25.0($\pm$0.1)°C in a thermostatic water-bath. Rod-like CT DNA samples ~200 bp in average length were prepared by sonication in order to minimize complexities arising from DNA flexibility [23]. Flow time was measured with a digital stopwatch, each sample was measured three times, and an average flow time was calculated. Data were presented as $(\eta/\eta_0)^{1/3}$ vs. binding ratio [24], where η is the viscosity of CT DNA in the presence of the Ru(II) complex and η_0 the viscosity of CT DNA alone.

Equilibrium dialysis and CD spectroscopy

Equilibrium dialyses were conducted with 5 ml of CT DNA (1.0 mM) sealed in a dialysis bag and 15 ml of complex (100 μM) outside the bag at 4°C. CD spectra of dialyzates of the complex were measured on a Jasco J-810 spectropolarimeter (Jasco Corporation, Tokyo, Japan) using a 0.1-cm path length cell at 25°C. The region between 220 and 350 nm was scanned for each sample three times. Blank controls of the complex were taken and no obvious signals were observed.

Cell viability assays

Human lung cancer cell line A549 and human embryonic lung fibroblast diploid normal cell line MRC-5 were cultured in Dulbecco's modified Eagle's medium (Thermo Scientific HyClone, Logan, USA) supplemented with 10% (v/v) fetal bovine serum (FBS) in 5% CO_2 atmosphere at 37°C, respectively. For cell viability assay, the cancer cells were plated at a density of 10^4 cells/well in 96-well plates (Iwaki; Asahi Technoglass, Gyouda, Japan) and incubated for 24 h. The medium was removed, and $[Ru(dmp)_2PMIP]^{2+}$ solutions were added into a new medium without FBS to the required final concentrations between 10 and 200 μM. The untreated A549 cells were used as a control.

After 72 h of incubation, 10 μl of a stock MTT solution was added to give a final concentration of 0.5 mg/ml and incubated for a further 4 h. Then, the medium was replaced with 100 μl of pure dimethyl sulfoxide and the absorbance of the dark blue formazan was measured with an ELISA plate reader at 570 nm. Cell viability = $(A_{sample}/A_{control}) \times 100\%$. MRC-5 cells were used as a control and treated by complex $[Ru(dmp)_2PMIP]^{2+}$ with the same procedures.

After 72 h of incubation with complex $[Ru(dmp)_2PMIP]^{2+}$, 30 μl of washed cell suspension was mixed thoroughly with 30 μl of trypan blue solution (0.4%) and allowed to stand for 3 min at room temperature. The total number of cells and the number of blue-stained cells (dead cells) were counted on a hemocytometer, using a microscope.

DNA content assay

DNA content was assayed as described previously [25]. Briefly, cells were treated with complex $[Ru(dmp)_2PMIP]^{2+}$ for 72 h, then collected at a density of ~10^6 cells/plate, rinsed with PBS buffer, and re-suspended in 70% ethanol overnight at 4°C. After centrifugation at 1000 rpm for 5 min, the samples were washed with PBS buffer twice, incubated in 1 ml PBS buffer (containing 50 μg/ml RNase, 37°C, 30 min), and then PI solution was added to cell suspensions to a final concentration of 50 μg/ml (dark, 4°C, 30 min). After filtration through a layer of 200-mesh silk screen, stained cells were analyzed on EPICS XL-MCL flow cytometer (Beckman Coulter, Fullerton, USA). The percentage of apoptotic cells was estimated using CellQuest program (Becton Dickinson, Franklin Lakes, USA).

Annexin V-FITC apoptosis detection assay

Apoptotic cells were detected by flow cytometry after staining with annexin V-FITC and PI using the annexin V-FITC apoptosis detection kit (BioVision, Mountain View, USA) as described previously [25]. Briefly, cells were treated with complex $[Ru(dmp)_2PMIP]^{2+}$ for 72 h, collected, washed with PBS buffer, and re-suspended in 500 μl of binding buffer containing 5 μl annexin V-FITC and 10 μl PI. After 5 min of incubation in darkness at room temperature, annexin V binding was analyzed by EPICS XL-MCL flow cytometer equipped with a FITC signal detector FL1 (excitation = 488 nm, green) and a PI signal detector FL2 (excitation = 488 nm, red). The percentage of apoptotic cells was calculated from the total (~10^4 cells) using EXPO32 MultiComp software (Beckman Coulter).

Statistical analysis

Data were expressed as mean $\pm$ SD of six to eight independent experiments. Statistical analyses were performed using Student's *t*-test. Values of $P < 0.05$ were considered to be statistically significant. The following notation was used throughout: $^*P < 0.05$ and $^{**}P < 0.01$, relative to control.

Results

DNA-binding properties

Figure 2(A) shows the ITC curves resulting from the injections of the Ru(II) complex into a solution of CT DNA at 25°C. The titration curves displayed that the binding reactions for CT DNA was exothermic, resulting in negative peaks in the plots of power vs. time. **Figure 2(B)** shows the plot of the heat evolved per mole of the Ru(II) complex added, corrected for the heat of Ru(II) complex dilution,

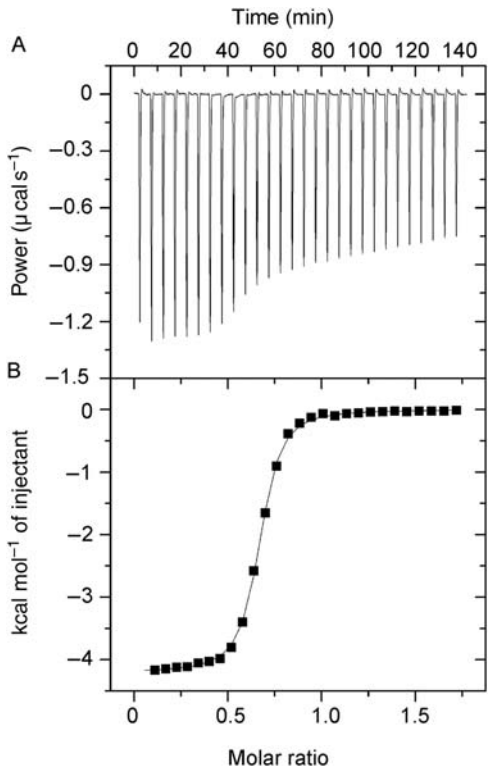

Figure 2 ITC profiles for the binding of complex $[Ru(dmp)_2PMIP]^{2+}$ to CT DNA at 25.0°C in HEPES buffer (20 mM, containing 0.1 mM EDTA, pH 7.2) (A) Raw data for sequential 10-μl injections of the Ru(II) polypyridyl complex (200 μM) into CT DNA (25.0 μM). (B) Plot of the heat evolved (kcal) per mole of Ru(II) complex added, corrected for the heat of Ru(II) complex dilution, against the molar ratio of the Ru(II) complex to CT DNA. The data (filled square) were fitted to a single set of identical sites model and the solid line represented the best fit.

against the molar ratio of the Ru(II) complex to CT DNA. The best fit for the integrated heat data was obtained using a single set of identical sites model with the lowest χ^2 (1.05 kcal mol^{-1}), yielding the thermodynamic parameters for the interactions of Ru(II) complex with CT DNA (**Table 1**). We further investigated the temperature dependence of the thermodynamic parameters for the binding reaction. A similar exothermic binding was observed for CT DNA at 20.0, 30.0, and 37.0°C, respectively.

The thermodynamic parameters for the binding reaction of CT DNA obtained at 20.0, 25.0, 30.0, and 37.0°C are summarized in **Table 1**. As shown in **Table 1**, the Ru(II) complex showed a strong and temperature-dependent binding affinity to CT DNA, and the binding constant decreased remarkably with the increase in the temperatures from 20.0 to 37.0°C. The binding of the complex to CT DNA was enthalpy- and entropy-driven reaction. Furthermore, the binding of complex $[Ru(dmp)_2PMIP]^{2+}$ to CT DNA showed strong temperature dependence of entropy and enthalpy changes and weak temperature dependence of Gibbs free energy change. From **Table 1**, it can also be seen that each complex bound to about two DNA bases. We have demonstrated that each of its analogue complex, $[Ru(phen)_2PMIP]^{2+}$, binds to about three DNA bases [7]. We suggested that the four methyl groups in the ancillary ligand of complex $[Ru(dmp)_2PMIP]^{2+}$ resulted in such a difference.

Figure 3 shows the temperature dependence of the standard thermodynamic parameters for the interaction of complex $[Ru(dmp)_2PMIP]^{2+}$ with CT DNA. As shown in **Fig. 3**, the molar heat capacity change associated with the binding of CT DNA, $\Delta_b C_{P,m}$, was -330.4 cal mol^{-1} K^{-1} for the plot of $\Delta_b H^0_m$ vs. T and -333.3 cal mol^{-1} K^{-1} for the plot of $\Delta_b S^0_m$ vs. ln T, respectively with linear correlation coefficients of 0.99. The values of $\Delta_b C_{P,m}$ obtained from both plots were similar to each other. The above results indicated that the molar heat capacity change of the binding reaction of CT DNA was independent of temperature in the range studied. A plot of $\Delta_b H^0_m$ vs. $T\Delta_b S^0_m$ for the binding reaction of CT DNA at different temperatures showed a slope of 1.03 with a linear correlation coefficient of 0.99 and an enthalpy intercept of -9.59 kcal mol^{-1}, indicating remarkable entropy–enthalpy compensation for CT DNA binding reaction.

Viscosity and CD spectroscopic studies

As shown in **Fig. 4**, the relative specific viscosity of DNA increased steadily with the increase in the concentration of

Table 1 Thermodynamic parameters for the binding of complex $[Ru(dmp)_2PMIP]^{2+}$ to CT DNA measured by ITC at different temperatures in 20 mM HEPES buffer (pH 7.2) containing 0.1 mM EDTA

T (°C)	n (bases/complex)	$K_b \times 10^{-6}$ (M^{-1})	$\Delta_b H^0_m$ (kcal mol^{-1})	$\Delta_b G^0_m$ (kcal mol^{-1})	$\Delta_b S^0_m$ (cal mol^{-1} K^{-1})
20.0	1.34 ± 0.01	10.20 ± 0.90	−2.42 ± 0.02	−9.41 ± 0.05	23.80 ± 0.23
25.0	1.55 ± 0.01	8.41 ± 0.38	−4.20 ± 0.01	−9.46 ± 0.03	17.60 ± 0.14
30.0	1.73 ± 0.01	7.60 ± 0.54	−5.57 ± 0.03	−9.55 ± 0.04	13.13 ± 0.25
37.0	1.94 ± 0.01	5.07 ± 0.24	−8.14 ± 0.03	−9.52 ± 0.03	4.48 ± 0.22

Thermodynamic parameters, K_b, $\Delta_b H^0_m$, and n, were determined using a single set of identical sites model. The standard molar-binding free energy ($\Delta_b G^0_m$) and the standard molar binding entropy ($\Delta_b S^0_m$) for the binding reaction were calculated using Equations (1) and (2), respectively. Errors shown are standard errors of the mean.

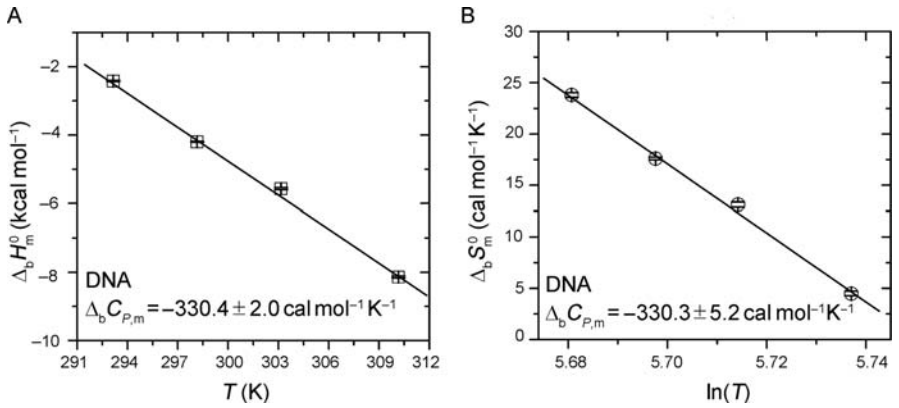

Figure 3 Temperature dependence of the standard molar enthalpy change and the standard molar entropy change for the binding of complex $[Ru(dmp)_2PMIP]^{2+}$ to CT DNA The molar heat capacity change associated with the binding reaction, $\Delta_b C_{P,m}$, was determined by linear regression analysis of the plot by $\Delta_b H^0_m = \Delta_b C_{P,m} T + \Delta H^0$ (A) and $\Delta_b S^0_m = \Delta_b C_{P,m} \ln T + \Delta S^0$ (B), respectively. Standard errors of the mean are shown.

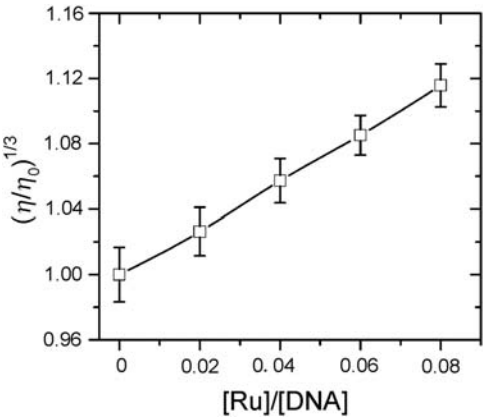

Figure 4 Effects of increasing concentrations of complex $[Ru(dmp)_2PMIP]^{2+}$ on the relative viscosities of CT DNA at 25.0°C in Tris–HCl buffer (5 mM, pH 7.2) The concentrations of CT DNA was 0.50 mM, and the molar ratios of the Ru(II) polypyridyl complex to CT DNA were 0.02, 0.04, 0.06, and 0.08, respectively. Data are expressed as mean ± SD ($n = 3$).

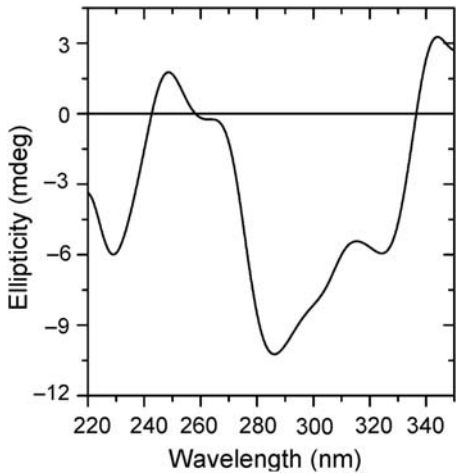

Figure 5 CD spectra of the dialyzates of complex $[Ru(dmp)_2PMIP]^{2+}$ after dialysis against CT DNA for 24 h The concentrations of CT DNA and the Ru(II) complex were 1 and 0.1 mM, respectively. Experiments were performed at 25°C.

Ru(II) complex, mainly for the lengthening of the DNA double helix resulting from intercalation [26,27].

Figure 5 shows the CD spectra in the UV region of the Ru(II) complex after its racemic solution had been dialyzed against CT DNA. As shown in **Fig. 5**, dialyzate of the Ru(II) complex showed two obvious CD signals, one is a positive peak at about 250 nm and the other is a negative peak at about 285 nm, indicating that the complex enantioselectively interacted with CT DNA.

Cytotoxicity studies

The cytotoxicity of complex $[Ru(dmp)_2PMIP]^{2+}$ to human lung tumor cells of A549 was measured by MTT reduction assay [28]. The metabolic activity of the cells was assessed by their ability to cleave the tetrazolium rings of the pale yellow MTT and form a dark blue water-insoluble formazan crystal. **Figure 6** shows the results of the cell viability experiments aimed at determining the cytotoxicity of complex $[Ru(dmp)_2PMIP]^{2+}$. As shown in **Fig. 6(A)**, complex $[Ru(dmp)_2PMIP]^{2+}$ showed significant dose-dependent cytotoxicity to human lung carcinoma cells of A549.

Because a potential anticancer drug candidate should selectively affect only tumor cells and not somatic cells [29], the cytotoxicity of complex $[Ru(dmp)_2PMIP]^{2+}$ to the normal diploid embryonic lung cell line (MRC-5) was also measured by MTT reduction assay. The complex showed preferential cytotoxicity to human lung tumor cells of A549 [**Fig. 6(A)**] vs. human lung normal cells of MRC-5 [**Fig. 6(B)**], indicating that the cytotoxic Ru(II) complex could be a potential anti-tumor drug.

We further employed trypan blue exclusion assay [30] to measure the cytotoxicity of complex $[Ru(dmp)_2PMIP]^{2+}$ to human lung tumor cells of A549.

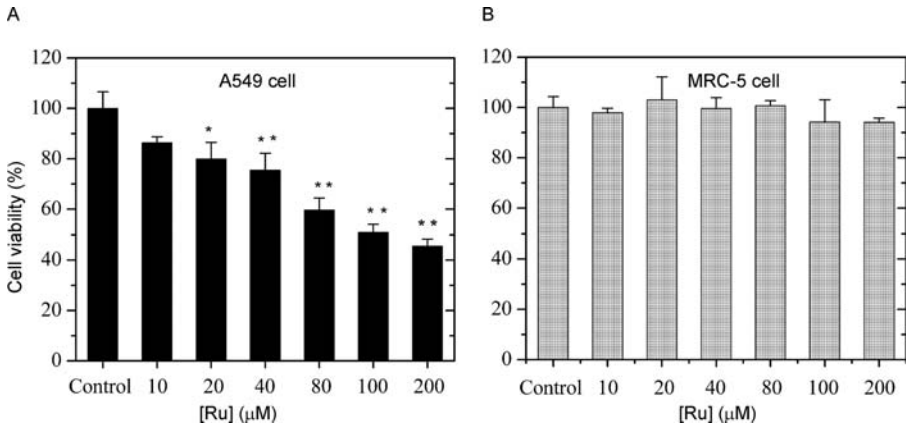

Figure 6 Cytotoxicity of complex $[Ru(dmp)_2PMIP]^{2+}$ to human lung tumor cells line A549 (A), compared with that to human embryonic lung fibroblast diploid normal cell line MRC-5 (B) Cytotoxicity was measured by MTT reduction assay. Cells were treated with complex $[Ru(dmp)_2PMIP]^{2+}$ at increasing complex concentrations using untreated cells as the control. Data are expressed as mean ± SD ($n = 6–8$). $^*P < 0.05$ and $^{**}P < 0.01$ vs. control.

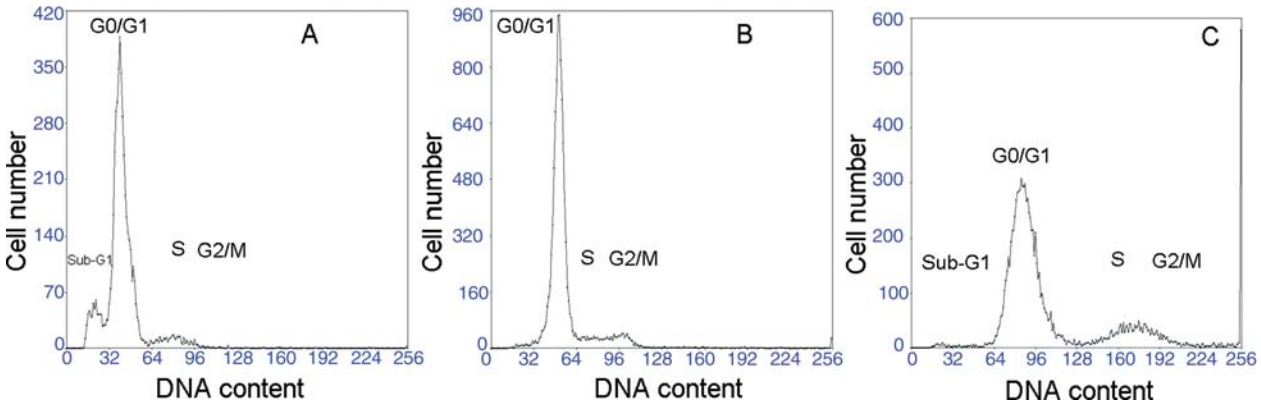

Figure 7 DNA content analyses of human lung cancer cell line A549 treated with complex $[Ru(dmp)_2PMIP]^{2+}$ on EPICS XL-MCL flow cytometer A549 cells (A) and MRC-5 cells (C) were treated with 80 μM $[Ru(dmp)_2PMIP]^{2+}$ for 72 h, respectively. (B) Untreated A549 cells. Sub-G1 peak is clearly evident in (A). The phases of the cell cycle from the left to the right were sub-G1-phase, G0/G1-phase, S-phase, and G2/M-phase.

Viable cells characterized by a structurally integral cell membrane do not uptake trypan blue dye. In contrast, dead cells (necrotic or late apoptotic cells) characterized by the loss of integrity of their membrane are stained blue by the dye [25,30]. At all concentrations tested, the Ru(II) complex reduced the number of viable A549 cells after staining with trypan blue at 72 h (effects on cell proliferation), which was much more evident at higher concentrations (120–200 μM) (data not shown), further supporting the conclusion reached by MTT reduction assay that such a complex shows significant dose-dependent cytotoxicity to A549 cells.

Apoptosis activity

Apoptotic cells show a reduced DNA content below the G0/G1 level. When apoptotic cells are stained by PI and analyzed by a flow cytometer, they display a broad hypodiploid (sub-G1) peak. Sub-G1 peak is one of the reliable biochemical markers of apoptosis [31], although the presence of a hypodiploid DNA peak is not a *bona fide* proof of apoptotic death [32]. Cytometric cell cycle analysis was performed by staining cells with PI and apoptosis was estimated by CellQuest program. **Figure 7(A)** shows the changes in DNA content distribution in human lung tumor cells of A549 treated by complex $[Ru(dmp)_2PMIP]^{2+}$ at IC_{50} concentration (80 μM), an equitoxic concentration. The percentage of apoptotic cells in A549 cells treated by the complex increased up to 11.8%, remarkably higher than those in untreated A549 cell line [0.7%, **Fig. 7(B)**] and in MRC-5 cell line treated by the complex at the same concentration [1.2%, **Fig. 7(C)**]. The DNA content frequency distribution histograms clearly indicated that the exposure of cells to the Ru(II) complex resulted in the appearance of cells with a fractional DNA content, which is defined as sub-G1 peak [**Fig. 7(A)**]. The above results indicated the cytotoxic Ru(II) complex induces apoptosis of human lung cancer cell line A549.

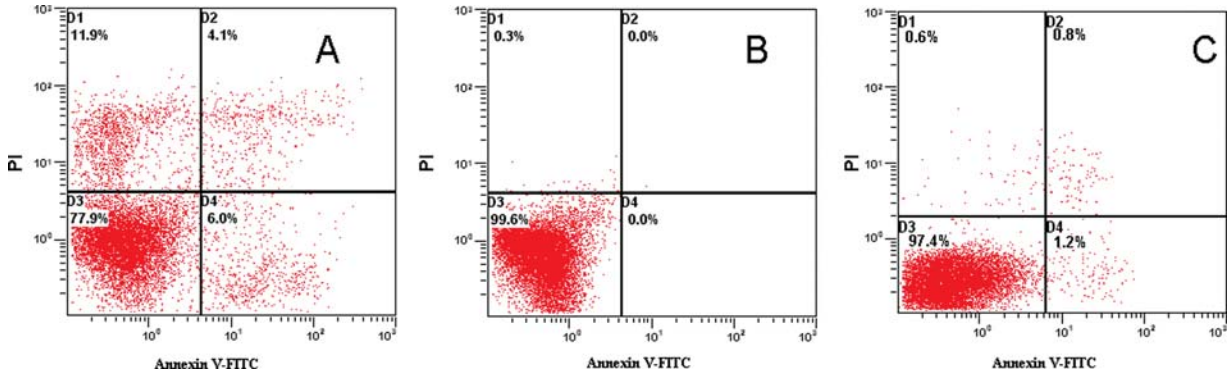

Figure 8 Annexin V staining shows induction of apoptosis A549 cells (A) and MRC-5 cells (C) were treated with 80 μM $[Ru(dmp)_2PMIP]^{2+}$ for 72 h, respectively. (B) Untreated A549 cells. The percents of apoptotic cells were detected by analyzing annexin V-FITC and PI binding with the help of flow cytometry and EXPO32 MultiComp software. Viable cells did not bind to annexin V or PI (lower left quadrant D3), early apoptotic cells bound to annexin V but excluded PI (lower right quadrant D4), and necrotic or late apoptotic cells were both annexin V- and PI-positive (upper right quadrant D2). The upper left quadrant D1 contains the cells damaged during the preparation of the cell suspension.

In the early stages of apoptosis, the cell membrane can expose phosphatidylserine which is annexin V-positive [32]. Phosphatidylserine externalization not only takes place in apoptosis, but also occurs during cell necrosis. The difference between these two forms of cell death is that during the early stages of apoptosis, the cell membrane remains intact, whereas at the very moment that necrosis occurs, the cell membrane looses its integrity and becomes leaky [33]. Therefore, the measurement of annexin V binding to the cell surface as indicative for apoptosis has to be performed in conjunction with a dye exclusion test to establish integrity of the cell membrane [33]. In combination with the membrane-impermeable DNA stain PI, with a flow cytometer, one can distinguish at least three different cell types during apoptosis: viable cells (annexin V- and PI-negative), early apoptotic cells (annexin V-positive but PI-negative), and necrotic or late apoptotic cells (annexin V- and PI-positive) [33,34]. In order to distinguish between apoptosis and necrosis, we performed double staining using annexin V-FITC and PI followed by flow cytometry. **Figure 8(A)** shows the effects of complex $[Ru(dmp)_2PMIP]^{2+}$ at IC_{50} concentration (80 μM) on apoptosis and necrosis in human lung tumor cells of A549. The percentage of early apoptotic cells in A549 cells treated by the Ru(II) complex was 6.0%, remarkably higher than those in untreated A549 cell line [0.0%, **Fig. 8(B)**] and in MRC-5 cell line treated by the complex at the same concentration [1.2%, **Fig. 8(C)**]. As shown in **Fig. 8**, 4.1% A549 cells treated by the Ru(II) complex were late apoptotic or necrotic, whereas almost no untreated A549 cells and only a very small amount of MRC-5 cells treated by the Ru(II) complex were late apoptotic or necrotic. Clearly, complex $[Ru(dmp)_2PMIP]^{2+}$ induced apoptosis of human lung tumor cell line A549. Our data here suggest that such a Ru(II) complex could be a potential anti-tumor drug.

Discussion

This study presented a detailed thermodynamic investigation on DNA binding of a Ru(II) complex containing a PMIP-intercalating ligand and two 2,9-dimethyl-1,10-phenanthroline ancillary ligands. Generally, thermodynamic-binding studies alone cannot establish the binding modes of a metal complex, so hydrodynamic studies, such as viscosity, sedimentation, and binding effects on DNA supercoiling, that are sensitive to length change and regarded as the most classical methods are needed to elucidate the intercalation modes of the octahedral complex $[Ru(dmp)_2PMIP]^{2+}$ to CT DNA. In this way, the viscosity measurement was carried out on CT DNA by varying the concentration of the Ru(II) complex. As expected, such a complex increased the relative specific viscosity of CT DNA steadily for the lengthening of the DNA double helix through the intercalation mode. Therefore, we concluded that complex $[Ru(dmp)_2PMIP]^{2+}$ intercalated into CT DNA base pairs in a way shown in **Fig. 9**. The role of Ru(II) here is to form a stable complex with a PMIP-intercalating ligand and two dmp ancillary ligands, accompanied by rich photophysical properties.

Molar heat capacity changes occurred in the binding reactions of biological molecules originate from the variations in non-polar and polar areas exposed to the solvent [18]. Both the standard molar enthalpy change and the standard molar entropy change for the binding strongly depended on temperature, yielding a negative molar heat capacity change of $-331.8\ cal\ mol^{-1}\ K^{-1}$ (average of the values from **Fig. 3**). Negative molar heat capacity change of the reaction demonstrated the burial of hydrophobic and hydrophilic solvent-accessible surface of CT DNA [35] upon interaction with the Ru(II) complex. Because of the presence of four methyl groups in the octahedral complex,

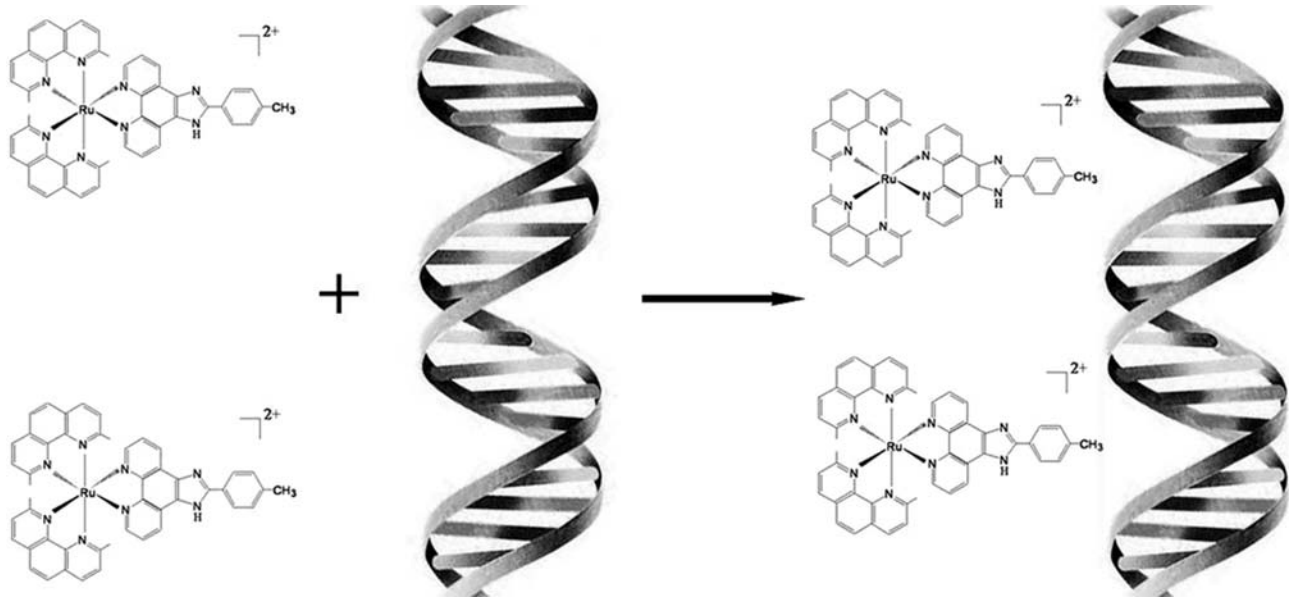

Figure 9 Schematic diagram illustrating complex $[Ru(dmp)_2PMIP]^{2+}$ intercalating into CT DNA base pairs

the majority of surface buried from exposure to solvent for this interaction could be hydrophobic rather than hydrophilic.

The enantiospecific binding of complex $[Ru(dmp)_2PMIP]^{2+}$ to CT DNA can be observed clearly from CD spectra. The presence of CD signals indicates enrichment of the enantiomer binding less favorably to CT DNA. From our CD experiments, we may deduce that although such a Ru(II) complex has not been resolved into its pure enantiomers, and we cannot determine which enantiomer binds to CT DNA enantioselectively experimentally, it is certain that the same isomer of the complex has a special preference for CT DNA binding. Barton [36] has brought forward the binding model that the Δ enantiomer of a metal complex will display a greater binding affinity with the right-handed CT DNA helix than the Λ enantiomer. Therefore, we deduce that the Δ enantiomer of the complex could bind more favorably to CT DNA and may be more effective for the cytotoxic action than the Λ enantiomer does.

Transition metal-based compounds such as Ru(II) complexes constitute a discrete class of chemotherapeutics, which are now used in the clinic as anti-tumor agents [4,5]. In the field of non-platinum compounds exhibiting anticancer properties, Ru(II) complexes are promising, showing activity on tumors which developed resistance to cisplatin or in which cisplatin is inactive [37,38]. Although the pharmacological target for Ru(II) compounds has not been unequivocally identified, there is a body of evidence indicating that the anti-tumor activity of Ru(II) complexes correlates with their ability to bind to DNA [13]. In the present study, complex $[Ru(dmp)_2PMIP]^{2+}$ bound to CT DNA with a strong and temperature-dependent binding affinity. The Ru(II) complex showed significant dose-dependent cytotoxicity to human lung tumor cells and induced apoptosis of human lung cancer cell line. But normal lung cells of MRC-5 were only slightly affected by the interaction of the Ru(II) complex with DNA in contrast to A549 tumor cells in the presence of the Ru(II) complex. It has been reported that the quercetin zinc(II) complex [39], hedamycin [40], and tris(tetramethylphenanthroline) Ru(II) [41] intercalate into the GC-rich core promoter region of survivin, down-regulating surviving gene expression and promoting tumor cells apoptosis. Therefore, we deduced that the Ru(II) complex intercalated into DNA and thereby induced apoptosis in tumor cells. It would be worthwhile to extend the current work to analyze caspase activation and/or the release of cytochrome *c* from mitochondria, typical of apoptotic cell death [42]. These are planned for the future.

In conclusion, we have investigated the interaction of the Ru(II) polypyridyl complex with CT DNA by using several biophysical methods and found that the complex intercalates into CT DNA, and hydrophobic and hydrophilic solvent-accessible surface of CT DNA is buried on complexation. Cell viability experiments indicate that the Ru(II) complex exhibits significant dose-dependent cytotoxicity to human lung tumor cells of A549. Further flow cytometry experiments show that the cytotoxic Ru(II) complex induces apoptosis of human lung cancer cell line A549. Our data demonstrate that the Ru(II) polypyridyl complex strongly binds to DNA and thereby induces apoptosis in tumor cells, suggesting that anti-tumor activity of the Ru(II) complex could be related to its interaction with DNA. Information obtained from this study will be helpful for designing new transition metal complexes used as potential anti-tumor drugs.

Acknowledgements

We sincerely thank Prof. Xiang Zhou and Dr Peng Hu (College of Chemistry and Molecular Sciences, Wuhan University) for their expert technical assistance on the synthesis of ruthenium(II) complexes and Prof. Hong Xu (College of Chemistry and Chemical Engineering, Shenzhen University) for his helpful suggestions.

Funding

This work was supported by National Key Basic Research Foundation of China Grant 2006CB910301, and National Natural Science Foundation of China Grants 30570421, 30770421, and 30970599.

References

1 Greguric I, Aldrich-Wright JR and Collins JG. A ^{1}H NMR study of the binding of Δ-[Ru(phen)$_2$DPQ]$^{2+}$ to the hexanucleotide d(GTCGAC)$_2$: evidence for intercalation from the minor groove. J Am Chem Soc 1997, 119: 3621–3622.

2 Nair RB, Teng ES, Kirkland SL and Murphy CJ. Synthesis and DNA-binding properties of [Ru(NH$_3$)$_4$dppz]$^{2+}$. Inorg Chem 1998, 37: 139–141.

3 Tan CP, Liu J, Chen LM, Shi S and Ji LN. Synthesis, structural characteristics, DNA binding properties and cytotoxicity studies of a series of Ru(III) complexes. J Inorg Biochem 2008, 102: 1644–1653.

4 Zhang CX and Lippard SJ. New metal complexes as potential therapeutics. Curr Opin Chem Biol 2003, 7: 481–489.

5 Kostova I. Ruthenium complexes as anticancer agents. Curr Med Chem 2006, 13: 1085–1107.

6 Xu H, Deng H, Zhang QL, Huang Y, Liu JZ and Ji LN. Synthesis and spectroscopic RNA binding studies of [Ru(phen)$_2$MHPIP]$^{2+}$. Inorg Chem Commun 2003, 6: 766–768.

7 Xu H, Liang Y, Zhang P, Du F, Zhou BR, Wu J and Liu JH, *et al*. Biophysical studies of a ruthenium(II) polypyridyl complex binding to DNA and RNA prove that nucleic acid structure has significant effects on binding behaviors. J Biol Inorg Chem 2005, 10: 529–538.

8 Kelland L. The resurgence of platinum-based cancer chemotherapy. Nat Rev Cancer 2007, 7: 573–584.

9 Brabec V. DNA modifications by antitumor platinum and ruthenium compounds: their recognition and repair. Prog Nucleic Acid Res Mol Biol 2002, 71: 1–68.

10 Nováková O, Kašpárková J, Vrána O, van Vliet PM, Reedijk J and Brabec V. Correlation between cytotoxicity and DNA binding of polypyridyl ruthenium complexes. Biochemistry 1995, 34: 12369–12378.

11 Alessio E, Mestroni G, Bergamo A and Sava G. Ruthenium antimetastatic agents. Curr Top Med Chem 2004, 4: 1525–1535.

12 Hartinger CG, Zorbas-Selfried S, Jakupee MA, Kynast B, Zorbas H and Keppler BK. From bench to bedside—preclinical and early clinical development of the anticancer agent indazolium trans-[tetrachlorobis(1H-indazole)ruthenate(III)] (KP1019 or FFC14A). J Inorg Biochem 2006, 100: 891–904.

13 Brabec V and Nováková O. DNA binding mode of ruthenium complexes and relationship to tumor cell toxicity. Drug Resist Update 2006, 9: 111–122.

14 Chaires JB. Energetics of drug-DNA interactions. Biopolymers 1998, 44: 201–215.

15 Haq I. Thermodynamics of drug-DNA interactions. Arch Biochem Biophys 2002, 403: 1–15.

16 Buurma NJ and Haq I. Advances in the analysis of isothermal titration calorimetry data for ligand-DNA interactions. Methods 2007, 42: 162–172.

17 Wu J, Du F, Zhang P, Khan IA, Chen J and Liang Y. Thermodynamics of the interaction of aluminum ions with DNA: implications for the biological function of aluminum. J Inorg Biochem 2005, 99: 1145–1154.

18 Liang Y. Applications of isothermal titration calorimetry in protein science. Acta Biochim Biophys Sin 2008, 40: 565–576.

19 Reichmann ME, Rice SA, Thomas CA and Doty P. A further examination of the molecular weight and size of desoxypentose nucleic acid. J Am Chem Soc 1954, 76: 3047–3053.

20 Amouyal E, Homsi A, Chambron JC and Sauvage JP. Synthesis and study of a mixed-ligand ruthenium(II) complex in its ground and excited states: bis(2,2-bipyridine)(dipyrido[3,2-a:2,3-c]phenazine-N^{4}N^5)ruthenium(II). Dalton Trans 1990, 6: 1841–1845.

21 Xiong Y, Zhou XH, Wu JH, Ji LN, Li RH, Zhou JY and Yu KB. Synthesis, structure and DNA-binding studies on the 2-(3-chlorophenyl) imidazo[4,5-f]1,10-phenanthroline-bis(2,2′-bipyridine)-ruthenium(II) complex. Transition Met Chem 1999, 24: 263–267.

22 van Holde KE, Johnson WE and Ho PS. Principles of Physical Biochemistry. Upper Saddle River: Pearson Prentice Hall, 2006.

23 Chaires JB, Dattagupta N and Crothers DM. Studies on interaction of anthracycline antibiotics and deoxyribonucleic acid: equilibrium binding studies on interaction of daunomycin with deoxyribonucleic acid. Biochemistry 1982, 21: 3933–3940.

24 Cohen G and Eisenberg H. Viscosity and sedimentation study of sonicated DNA-proflavine complexes. Biopolymers 1969, 8: 45–55.

25 Zhang M, Yang F, Jr, Yang F, Chen J, Zheng CY and Liang Y. Cytotoxic aggregates of α-lactalbumin induced by unsaturated fatty acid induce apoptosis in tumor cells. Chem Biol Interact 2009, 180: 131–142.

26 Satyanarayana S, Dabrowiak JC and Chaires JB. Neither Δ- nor Λ-tris(phenanthroline)ruthenium(II) binds to DNA by classical intercalation. Biochemistry 1992, 31: 9319–9324.

27 Satyanarayana S, Dabrowiak JC and Chaires JB. Tris(phenanthroline) ruthenium(II) enantiomer interactions with DNA: mode and specificity of binding. Biochemistry 1993, 32: 2573–2584.

28 Mosmann T. Rapid colorimetric assay for cellular growth and survival: application to proliferation and cytotoxicity assays. J Immunol Methods 1983, 65: 55–63.

29 Tseng CH, Chen YL, Chung KY, Cheng CM, Wang CH and Tzeng CC. Synthesis and antiproliferative evaluation of 6-arylindeno[1,2-c]quinoline derivatives. Bioorg Med Chem 2009, 17: 7465–7476.

30 Katsarou ME, Efthimiadou EK, Psomas G, Karaliota A and Vourloumis D. Novel copper(II) complex of *N*-propyl-norfloxacin and 1,10-phenanthroline with enhanced antileukemic and DNA nuclease activities. J Med Chem 2008, 51: 470–478.

31 Darzynkiewicz Z, Robinson PJ and Crissman HA. Flow Cytometry. New York: Academic Press, 1994.

32 Riccardi C and Nicoletti I. Analysis of apoptosis by propidium iodide staining and flow cytometry. Nat Protoc 2006, 1: 1458–1461.

33 Vermes I, Haanen C, Steffens-Nakken H and Reutelingsperger C. A novel assay for apoptosis: flow cytometric detection of phosphatidylserine expression on early apoptotic cells using fluorescein labelled annexin V. J Immunol Methods 1995, 184: 39–51.

34 Bhattacharjee RN, Park KS, Kumagai Y, Okada K, Yamamoto M, Uematsu S and Matsui K, *et al*. VP1686, a Vibrio type III secretion protein, induces toll-like receptor-independent apoptosis in macrophage through NF-κB Inhibition. J Biol Chem 2006, 281: 36897–36904.

35 Haq I, Ladbury JE, Chowdhry BZ, Jenkins TC and Chaires JB. Specific binding of hoechst 33258 to the d(CGCAAATTTGCG)$_2$ duplex: calorimetric and spectroscopic studies. J Mol Biol 1997, 271: 244–257.

36 Barton JK. Metals and DNA: molecular left-handed complements. Science 1986, 233: 727–734.

37 Messori L, Orioli P, Vullo D, Alessio E and Lengo E. A spectroscopic study of the reaction of NAMI, a novel ruthenium(III)anti-neoplastic complex, with bovine serum albumin. Eur J Biochem 2000, 267: 1206–1213.

38 Rademaker-Lakhai JM, van den Bongard D, Pluim D, Beijnen JH and Schellens JHM. A Phase I and pharmacological study with imidazolium-trans-DMSO-imidazole-tetrachlororuthenate, a novel ruthenium anticancer agent. Clin Cancer Res 2004, 10: 3717–3727.

39 Tan J, Wang BC and Zhu LC. DNA binding, cytotoxicity, apoptotic inducing activity, and molecular modeling study of quercetin zinc(II) complex. Bioorg Med Chem 2009, 17: 614–620.

40 Wu JG, Ling X, Pan DL, Pasha A, Song L, Liang P and Altieri DC, *et al*. Molecular mechanism of inhibition of survivin transcription by the GC-rich sequence-selective DNA binding antitumor agent, hedamycin. J Biol Chem 2005, 280: 9745–9751.

41 Mei HY and Barton JK. Tris(tetramethylphenanthroline)ruthenium(II): a chiral probe that cleaves A-DNA conformations. Proc Natl Acad Sci USA 1988, 85: 1339–1343.

42 Chen SH, Lin JK, Liang YC, Pan MH, Liu SH and Lin-Shiau SY. Involvement of activating transcription factors JNK, NF-κB, and AP-1 in apoptosis induced by pyrrolidine dithiocarbamate/Cu complex. Eur J Pharmacol 2008, 594: 9–17.